ORIGINAL PAPER

CrossMark

Thermal stability of catalyst for ammonia synthesis based on cobalt molybdenum nitrides

Paweł Adamski[1] · Dariusz Moszyński[1] · Marlena Nadziejko[1] · Agata Komorowska[1] · Adam Sarnecki[1] ·
Aleksander Albrecht[1]

Abstract

The formation and stability of an ammonia synthesis catalyst, based on cobalt molybdenum nitrides, were studied. The activation process of the catalyst was examined by in situ X-ray diffractometry. The thermal stability of obtained active phase of the catalyst was tested at 700 °C under ammonia atmosphere, N_2/H_2 mixture and under pure hydrogen. The presence of Co_2Mo_3N and Co_3Mo_3N phases in the catalyst was confirmed. The phase composition was stable in a long-term test performed under nitrogen/hydrogen atmosphere. Co_3Mo_3N phase decomposed into Co_6Mo_6N after exposure to pure hydrogen.

Keywords Cobalt molybdenum nitrides · Ammonia synthesis · Thermal stability

Introduction

During the twentieth century, world production rate of ammonia has considerably grown. Currently ammonia, apart from petrochemicals, is one of the most produced chemicals. High temperature and pressure required for ammonia synthesis significantly affect world energy consumption. The energy expenditure of ammonia synthesis is largely a consequence of the steam reforming process used for H_2 production. However, the energy savings in an ammonia synthesis loop are of great importance. Therefore, a continuous effort to improve the Haber–Bosch process and develop new catalysts is being devoted. At the beginning of the twenty-first century, several new catalysts mostly based on cobalt compounds were presented (Hargreaves 2014; Jacobsen 2000; Kojima and Aika 2001a; McAulay et al. 2015; Moszyński et al. 2010, 2015, 2018; Tarka et al. 2015, 2017; Zybert et al. 2016). Among this materials, cobalt molybdenum nitrides

✉ Dariusz Moszyński
dmoszynski@zut.edu.pl

1 Faculty of Chemical Technology and Engineering, Institute of Inorganic Chemical Technology and Environment Engineering, West Pomeranian University of Technology, Szczecin, Pułaskiego 10, 70-322 Szczecin, Poland

are considered as a possible replacement for the commercial multi-promoted iron catalyst.

Theoretical studies based on microkinetic calculations suggested that there is a volcano-shape relation between the ammonia synthesis activity of different materials and their nitrogen adsorption energy (Dahl et al. 2001). The existence of such volcano plot implies that there is an optimum, which compromise two different ways of achieving high activity in ammonia synthesis, namely a low energy for activation of nitrogen dissociation and a low concentration of active sites occupied by nitrogen. According to the mentioned theoretical studies, element combination, which fulfills these requirements and has the highest turnover frequencies for ammonia synthesis was found to be cobalt–molybdenum (Jacobsen et al. 2001).

Chemical compounds with cobalt and molybdenum atoms in their structure and reportedly having a high activity in the ammonia synthesis process are cobalt molybdenum nitrides. Cobalt molybdenum nitrides occur in three stable crystallographic forms Co_3Mo_3N, Co_2Mo_3N and Co_6Mo_6N. Co_3Mo_3N is isostructural with -Fe_3W_3C (-6 carbide structure), which crystallizes with cubic symmetry in the space group Fd$\bar{3}$m, and lattice parameter $a = 11.0270$ Å (Jackson et al. 1999). In the Co_3Mo_3N structure, Mo atoms occupy the 48f position, Co atoms 32e and 16d positions, nitrogen atoms 16c position. The structure consists of corner-shared Mo_6N octahedra with Co atoms occupying the sites between the octahedra. Co_2Mo_3N is isostructural with the

filled β-manganese structure, which crystallizes with cubic symmetry in the space group P4$_1$32, and lattice parameter $a = 6.6653$ Å (Prior and Battle 2003). This structure contains a net of cobalt atoms and the holes which are filled by Mo$_6$N octahedra. In the Co$_2$Mo$_3$N structure, Mo atoms occupy the 12d position, Co atoms 8c position and N atoms 4a position. Co$_2$Mo$_3$N has been only obtained in mixtures with Co$_3$Mo$_3$N. Co$_6$Mo$_6$N crystallizes with cubic symmetry and has space group—Fd$\bar{3}$m, and lattice parameter $a = 10.8824$ Å (Hunter et al. 2010). Co$_6$Mo$_6$N has -12 carbide structure, in which Co atoms are placed in the 32e and 16d sites, Mo atoms occupy the 48f sites and nitrogen atoms are exclusively located at the 8a sites, as opposed to the 16c sites occupied by N atoms in Co$_3$Mo$_3$N phase.

Co$_3$Mo$_3$N at 700 °C can be converted into Co$_6$Mo$_6$N in the presence of hydrogen through a loss of 50% of the lattice nitrogen (Hunter et al. 2010). This transformation is reversible. In the presence of nitrogen or ammonia, Co$_3$Mo$_3$N structure is recreated (Gregory et al. 2011). The ability of cobalt molybdenum nitrides to reversibly transform to nitrogen-rich or -lean phase led to their potential application as nitrogen transfer reagents (Mckay et al. 2007). This phenomenon is explained in terms of the Mars–van Krevelen mechanism. In the presence of hydrogen, lattice N species undergo reaction to yield NH$_3$. Furthermore, if nitrogen is present in the atmosphere, the nitrogen vacancies in the nitride lattice are replenished. Relocation of nitrogen occurs from the 16c site in the Co$_3$Mo$_3$N lattice to the 8a site in the Co$_6$Mo$_6$N lattice.

Co$_3$Mo$_3$N obtained via ammonolysis from cobalt molybdate hydrate is more active in ammonia synthesis process than the commercial multi-promoted iron catalyst (Kojima and Aika 2001a). Additional promotion with alkali metals results in a further increase of Co$_3$Mo$_3$N activity (Kojima and Aika 2001a). Alkali metals act as electronic promoters, donating an electron to the catalyst active center. As an unfavorable effect of alkali addition, a decrease of the surface area is observed (Kojima and Aika 2001b; Moszyński et al. 2015).

The promotion with cesium or potassium compounds inhibits the formation of pure Co$_3$Mo$_3$N and the mixture of Co$_2$Mo$_3$N and Co$_3$Mo$_3$N is formed (Moszyński 2013; Moszyński et al. 2010, 2015). The promoter concentration influences the phase composition of considered catalysts. Co$_3$Mo$_3$N–Co$_2$Mo$_3$N ratio decreases with the increase of alkali concentration, but above a certain threshold, starts to increase again. Doping of cobalt molybdenum nitrides with chromium compounds results in reverse dependency: chromium limits the formation of Co$_2$Mo$_3$N and increases Co$_3$Mo$_3$N–Co$_2$Mo$_3$N ratio. Double promotion with potassium and chromium results in the formation of more active and stable material (Moszyński et al. 2018). Chromium is considered as a structural promoter, which enhances surface stability and increases the specific surface area of the catalyst. Despite the high activity, the application of cobalt molybdenum nitrides in the industry is limited by their low operational parameters, like thermal stability and activity maintenance during the long catalytic process. Development of an efficient strategy to counteract this adverse effect is a critical factor for further applications of cobalt molybdenum nitrides.

In this study, the thermal stability of the nonpromoted catalyst during the ammonia synthesis process was carefully examined via in situ powder X-ray diffraction (PXD) studies. Simulation of conditions similar to this applied in the industrial practice was conducted. Furthermore, prolonged heat treatment to simulate the aging of the catalyst was performed and the stability of the catalyst under a hydrogen atmosphere was examined.

Experimental

The precursor of the catalyst was prepared by a multi-step procedure consisting of precipitation, filtration and drying. Hot water solutions of cobalt(II) nitrate [Co(NO$_3$)$_2$·6H$_2$O] and ammonium heptamolybdate [(NH$_4$)$_6$Mo$_7$O$_{24}$· 4H$_2$O] were mixed. The chemicals used were of an analytical grade (Chempur, Poland). The resulting solution was heated up to 90 °C. A purple precipitate was obtained after vacuum filtration and it was rinsed twice with distilled water and once with ethanol. The obtained powder was dried overnight at 150 °C and ground in an agate mortar.

The chemical composition of the precursor was determined with the use of inductively coupled plasma atomic emission spectroscopy ICP-AES (Perkin-Elmer Optima 5300 DV). Co/Mo composition of the precursor was ascertained as 1.07.

Phase transformations occurring during activation and the ammonia synthesis process as well as catalyst stability were thoroughly studied via in situ PXD. The precursor was placed on the rigid sample holder, which was mounted in the Anton Paar XRK 900 reaction chamber. The volume of the reaction chamber was 400 cm^3 and the time needed to flush the reaction chamber completely was estimated to be 10 min (with the flow 100 cm^3/min). Gas atmosphere in the reaction chamber was controlled by Brooks SLA flow regulators. Gas connections used in the experimental setup were Swagelok type (made from 316 stainless steel). The phase composition of the precursor and catalyst was analyzed by Philips X'pert MPD powder diffractometer. The apparatus worked in Bragg–Brentano geometry and a copper Kα radiation source was used ($\lambda_{\alpha1} = 0.154056$ nm, $\lambda_{\alpha2} = 0.154439$ nm). Scans were collected with a hybrid PIXcel[1D] detector. In the incident beam path, nickel filter with 0.02 mm thickness was applied, while in the diffracted beam path, curved graphite

crystal monochromator in (002) position was used. Diffraction data were recorded in diffraction angle ranges between 20 and 60° 2θ, with 0.02 step size and collection time of approximately 0.8 s per step.

Phase analysis was performed with the International Centre for Diffraction Data ICDD PDF-4+ database. A full-pattern fit based on the Rietveld method was conducted to calculate the weight fractions of the crystallographic phases identified in the material. A semi-automatic procedure of Rietveld refinement included in the HighScore Plus 3.0e software by PANalytical was used. During this procedure, the following parameters were varied: scale factors, unit cell dimensions, atom coordinates, occupancy factors, peak profile shape and full width at half maximum (FWHM). All initial crystal data required for Rietveld refinement were retrieved from the ICDD PDF-4+ database.

Applied experimental conditions were as similar to the real activation and ammonia synthesis process as possible. The course of the process is presented in Fig. 1. The diffraction pattern at ambient conditions was acquired. The sample was heated to 700 °C in the nitrogen (99.999 vol%) 100 cm^3/min flow. Subsequent PXD scan was performed. Activation of the precursor was carried out via ammonolysis in the pure ammonia (99.98 vol%) 100 cm^3/min flow. The diffraction patterns were constantly collected during ammonolysis. In the next step, reaction gas was changed to the mixture of nitrogen (99.999 vol%) and hydrogen (99.999 vol%), with flows 25 cm^3/min and 75 cm^3/min, respectively. The gas components ratio was used to imitate real ammonia synthesis conditions. Temperature program performed in the

present study allowed simulating the influence of different gas atmospheres on the structural properties of the material. The temperature of 700 °C is required to carry out the ammonolysis of the catalyst precursor. Industrial process of ammonia synthesis is generally performed in the range 400–500 °C. The experiment was intended to simulate a prolonged stability test. Therefore, the temperature used throughout the ammonia synthesis stage was also 700 °C. The limitation to presented reaction setup is high pressure required to increase the conversion rate in the industrial process, which cannot be applied in the used equipment. In the last step, pure hydrogen (99.999 vol%) 100 cm^3/min flow was passing through the reaction chamber. Stability of the sample at reduction conditions was examined.

Results and discussion

The precursor of the catalyst was obtained by precipitation from water solutions of cobalt and molybdenum salts followed by filtration and drying. The only crystalline phase identified in the precursor is cobalt molybdate hydrate, $CoMoO_4$ $3/4H_2O$. A detailed analysis of the precursor composition was given in (Moszyński et al. 2015, 2018).

The precursor was exposed to the nitrogen atmosphere and heated in the reactor chamber of the diffractometer. At the temperature of 700 °C, the X-ray diffraction analysis revealed the presence of two crystalline phases, namely $Co_2Mo_3O_8$ (ICDD No. 04-001-9062) (Tourne and Czeskleba 1970) and metallic cobalt (ICDD No. 04-006-4263) (Jarlborg

Fig. 1 The course of the processes performed in the reaction chamber. A—Annealing at 700 °C (100 vol% N_2), B—ammonolysis at 700 °C (100 vol% NH_3), C—ammonia synthesis at 700 °C (25 vol% N_2 + 75 vol% H_2), D—reduction at 700 °C (100 vol% H_2)
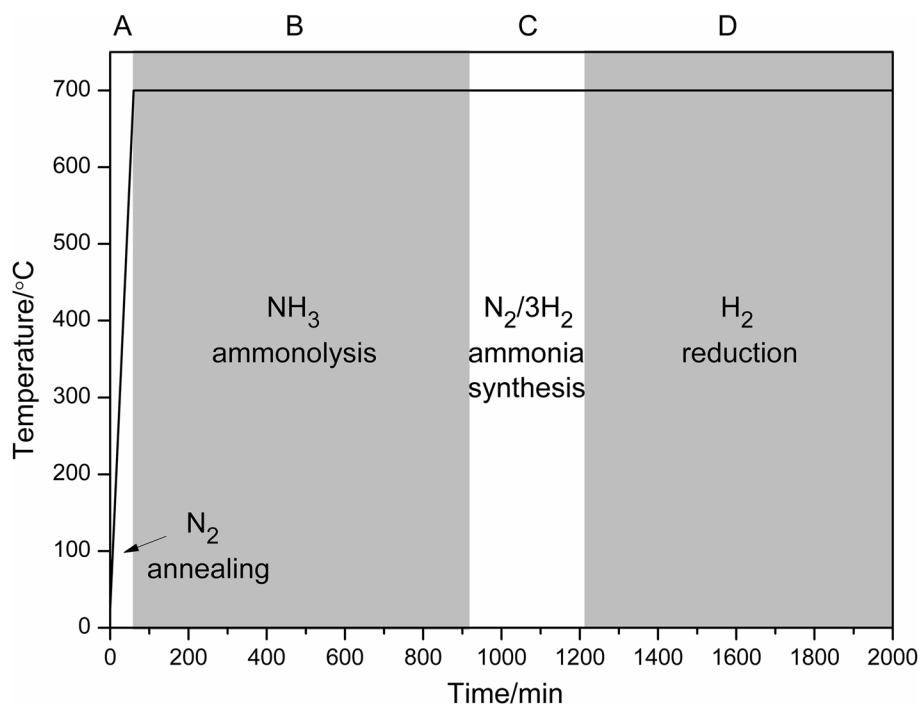
and Peter 1984) (Fig. 2). Low-intensity reflections located at approximately 27°, 31°, 42° and 48° 2θ can be observed in Fig. 2. Possibly, these reflections originate from faulted intermediate phase—CoMoO$_4$. The heating of the precursor apparently results in its dehydration to CoMoO$_4$ oxide. The estimated composition of the product observed by PXD based on Rietveld analysis is 90 wt% of Co$_2$Mo$_3$O$_8$ and 10 wt% of Co. Since CoMoO$_4$ phase is of very low intensity, it was not considered in the Rietveld analysis. CoMoO$_4$ at 700 °C under a nitrogen atmosphere is decomposed to oxide-lean phase, following the reaction below:

$$3CoMoO_4 \rightarrow Co_2Mo_3O_8 + Co + 2O_2 \qquad (1)$$
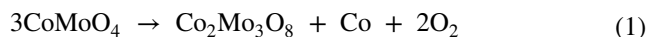
Regarding thermodynamics of the ternary Co–Mo–O system studied at 927 °C (Jacob and Vana Varamban 1998), the decomposition of CoMoO$_4$ oxide should follow the reaction shown below:

$$2CoMoO_4 \rightarrow 2/3Co_2Mo_3O_8 + 2/3CoO + O_2 \qquad (2)$$
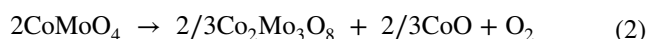
According to (Eq. 2) the occurrence of CoO phase, which was not confirmed by PXD analysis, is expected. Under the very low partial pressure of oxygen, the formation of the Co$_{0.97}$Mo$_{0.03}$ alloy was reported (Jacob and Vana Varamban 1998). The presence of the metallic Co was identified on the basis of diffraction pattern acquired at 700 °C. Therefore, the thermal shift of diffraction patterns due to thermal expansion of the crystallographic lattice is anticipated. In the present study, an observed shift between exemplary reflections from patterns identified as originating from Co$_2$Mo$_3$O$_8$ and Co phases is as follows: (a) Co$_2$Mo$_3$O$_8$—reflection at 45.460° (shifted by 0.025° 2θ), (b) Co—reflection at 43.990° (shifted 0.295° 2θ). Since in general, thermal expansion of oxides

is much smaller than metallic phases, observed shifts are plausible. Due to the observed shift, the difference between diffraction patterns of metallic Co and molybdenum-lean Co–Mo alloys seems to be impossible to differentiate. It must be admitted that an excess of cobalt atoms was found in the precursor (molar ratio of Co/Mo atoms in the precursor is 1.07). Therefore, it cannot be excluded that the Co phase identified in the diffraction patterns may be a lean Co–Mo alloy.

The catalysts considered to be applicable in the ammonia synthesis process are active in their metallic forms. They are also susceptible to oxidation under air. Therefore, their activation from the precursor is usually performed in the ammonia synthesis reactor. This process was simulated in the reaction chamber of the diffractometer. The ammonolysis process was carried out at 700 °C under pure ammonia. The final product observed after 800 min of the process was identified as a mixture of two ternary nitride phases: Co$_2$Mo$_3$N (ICDD No. 04-010-6426) (Prior and Battle 2003) and Co$_3$Mo$_3$N (ICDD No. 04-008-1301) (Jackson et al. 1999) with a small component of metallic Co (Fig. 3). There is a characteristic group of three reflections attributed to Co$_2$Mo$_3$N and other characteristic group attributed to Co$_3$Mo$_3$N. There are reflections at approximately 40.5°, 42.9° and 45.1° 2θ originating from the former phase and reflections at 40.0°, 42.6° and 46.5° 2θ for the latter phase. In the initial stage of the ammonolysis besides the formation of Co$_2$Mo$_3$N and Co$_3$Mo$_3$N nitrides, the disappearance of Co$_2$Mo$_3$O$_8$ and the decrease of metallic cobalt concentration were observed. Apparently, Co$_2$Mo$_3$O$_8$ and Co phases are intermediates of the final product and plausible chemical reactions occurring during ammonolysis are:

Fig. 2 The diffraction pattern of the sample after annealing at 700 °C. Reflections ascribed to identified phases are indicated by bars under diffraction pattern
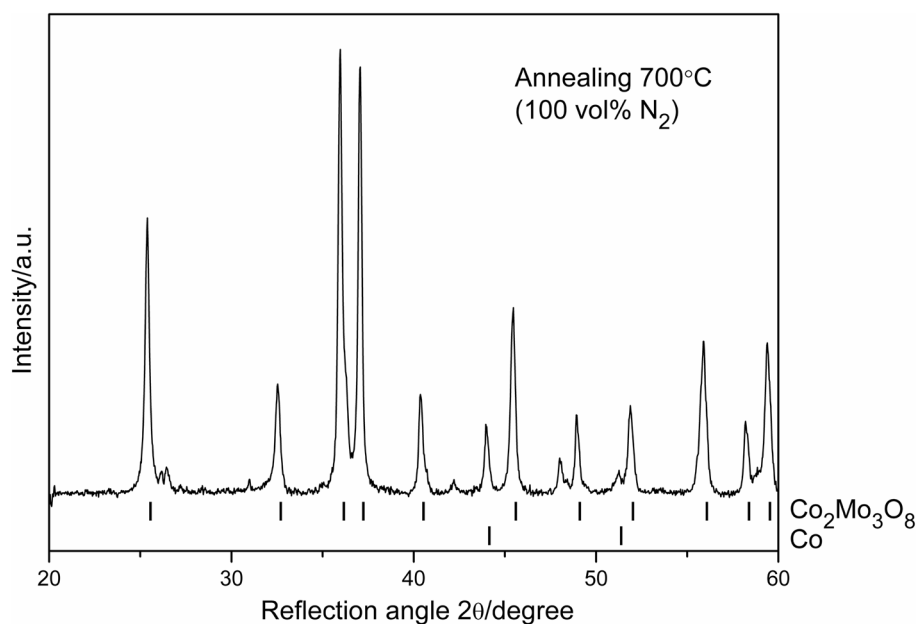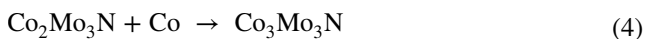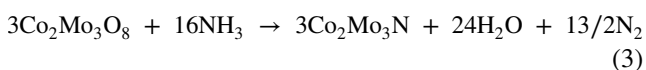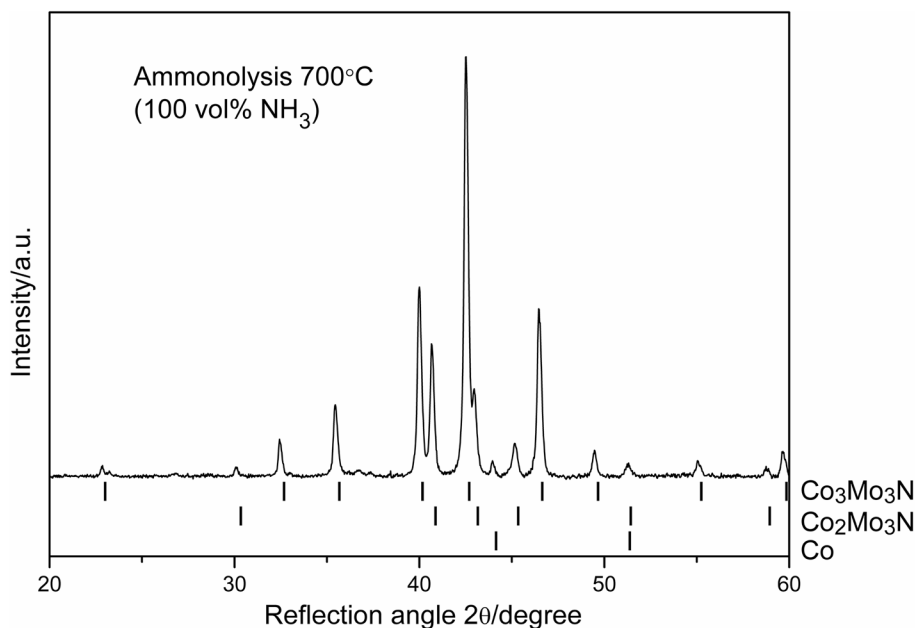
Fig. 3 The diffraction pattern of the sample at a late stage of ammonolysis. Reflections ascribed to identified phases are indicated by bars under diffraction pattern

$$3Co_2Mo_3O_8 + 16NH_3 \rightarrow 3Co_2Mo_3N + 24H_2O + 13/2N_2 \tag{3}$$

$$Co_2Mo_3N + Co \rightarrow Co_3Mo_3N \tag{4}$$

In the next stage of the experiment, thermal stability under the ammonia synthesis conditions was simulated. The catalyst was exposed to the nitrogen–hydrogen mixture (25 vol%. N_2–75 vol% H_2) at 700 °C. The PXD observations performed in this stage showed minor differences between the diffraction patterns. The only significant effect observed during this stage is the total disappearance of metallic Co. Co_2Mo_3N and Co_3Mo_3N mixture present under ammonia synthesis conditions is a stable form of the catalyst.

In the last stage of the experiment, the catalyst was exposed to the pure hydrogen. It was still kept at 700 °C and diffraction patterns were acquired for a prolonged period. A significant effect of this process is formation of Co_6Mo_6N phase (see Fig. 4) (ICDD No. 04-017-2710) (Hunter et al. 2010). Reflections characteristic for this phase are positioned at 40.7°, 43.3° and 47.3° 2θ. The reduction was being conducted for about 1000 min. During this process, increase of

Fig. 4 The diffraction pattern of the sample during the reduction step. Reflections ascribed to identified phases are indicated by bars under diffraction pattern
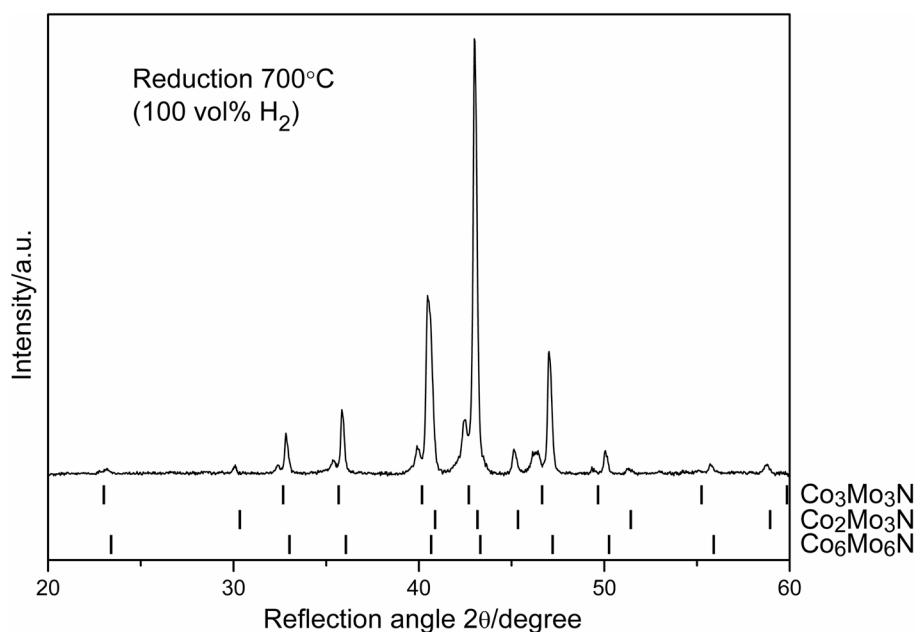
Co_6Mo_6N phase concentration was observed. It is noteworthy that generally, only the concentration of Co_3Mo_3N was being decreased during this stage of the experiment. Regarding experimental errors, the concentration of Co_2Mo_3N phase was stable till the end of the experiment. This observation suggests that the transformation of Co_3Mo_3N phase into Co_6Mo_6N phase was being taken place in this stage. The final composition of the catalyst after the experiment was approximately 15 wt% of Co_2Mo_3N, 15 wt% of Co_3Mo_3N and 70 wt% of Co_6Mo_6N.

The contour plot of diffraction lines displaying an evolution of the material under different gas atmospheres is shown in Fig. 5. The higher density of isolines means the higher intensity of particular diffraction line. To eliminate background noise, only lines with an intensity of 30% (relative to the most intense line) or higher are visible. Furthermore, the 2θ range is narrowed to make the graph more readable. Transitions of the position of diffraction lines occurred only at ammonolysis and reduction stages. No transitions of diffraction lines during ammonia synthesis were observed. For example, the introduction of ammonia at B stage of the experiment resulted in a shift of diffraction line from 36° to 35.5° 2θ and appearance of new diffraction lines at 40°, 40.5° and around 42.5° and 43° 2θ. Also, lines at 37°, 40.5° and 44° 2θ disappeared. The evolution of the phase composition during the process is shown in Fig. 6.

Regarding the presented data, a course of the experiment can be proposed (Fig. 7). The annealing of $CoMoO_4·3/4H_2O$

under pure nitrogen results in the decomposition of that oxide to a mixture consisting of approximately 90 wt% of $Co_2Mo_3O_8$ and 10 wt% of Co. This process is supposedly preceded by dehydration of the $CoMoO_4·3/4H_2O$. Under the ammonia atmosphere, the mixture of $Co_2Mo_3O_8$ and metallic Co gradually transforms into a mixture of cobalt molybdenum nitrides: Co_2Mo_3N and Co_3Mo_3N. This material is considered as an active form of the catalyst and consists of approximately 80 wt% of Co_3Mo_3N and 20 wt% of Co_2Mo_3N. The catalyst was stable under ammonia synthesis conditions even though the process was carried out at a much higher temperature than required for efficient ammonia production. The performed experiment was designed to simulate thermal stability of the material. However, it is hard to evaluate stability of the catalyst at the real industry conditions, because the material was examined only at the laboratory scale. Further research of the nitride system in the larger scale (semi-technical) is required to make the conclusions. Under a hydrogen atmosphere, Co_3Mo_3N is converted into nitrogen-lean phase Co_6Mo_6N. Under reducing conditions, Co_2Mo_3N phase remains stable and constitutes about 15–20 wt% of the material.

Stability data presented in this article could be useful to tailor new catalysts made of ternary and quaternary nitrides. Furthermore, comparison of already studied materials could be very fruitful. For instance, the cobalt molybdenum nitrides catalyst compared to a nickel molybdenum nitride catalyst known from the literature undergoes different

Fig. 5 The contour plot of diffraction lines changing with the time of the experiment. A—Annealing at 700 °C (100 vol% N_2), B—ammonolysis at 700 °C (100 vol% NH_3), C—ammonia synthesis at 700 °C (25 vol% N_2 + 75 vol% H_2), D—reduction at 700 °C (100 vol% H_2)
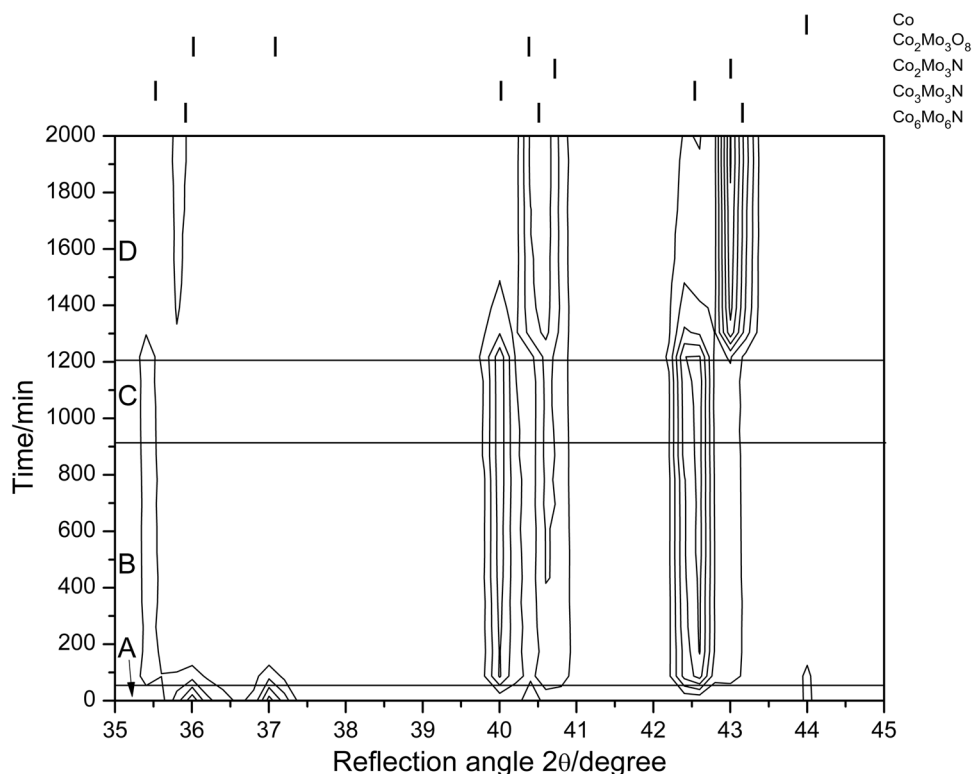
Fig. 6 Evolution of the phase composition of the sample during the experiment performed in the reaction chamber of the diffractometer. A—Annealing at 700 °C (100 vol% N_2), B—ammonolysis at 700 °C (100 vol% NH_3), C—ammonia synthesis at 700 °C (25 vol% N_2 + 75 vol% H_2), D—reduction at 700 °C (100 vol% H_2)
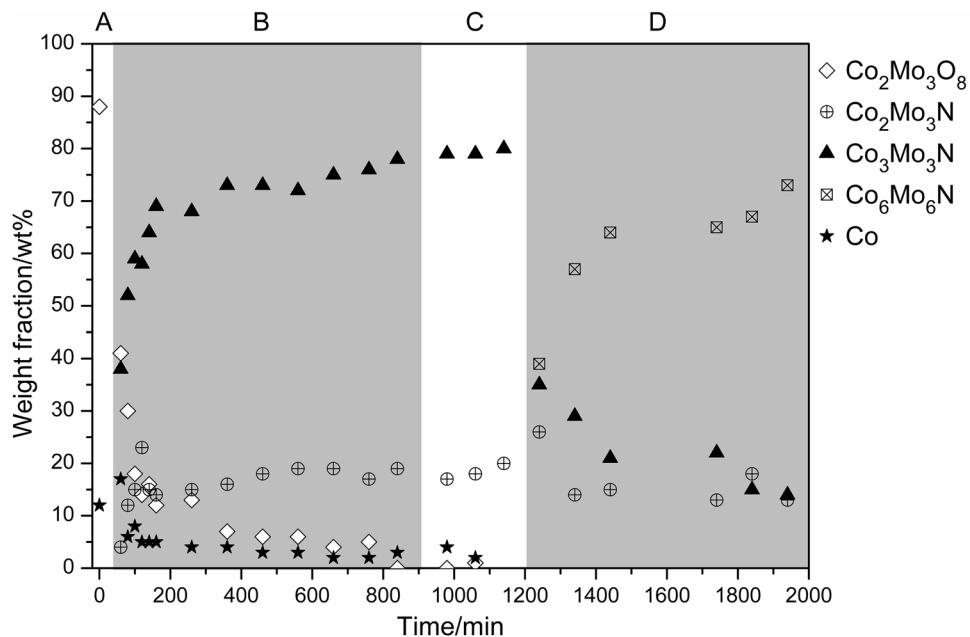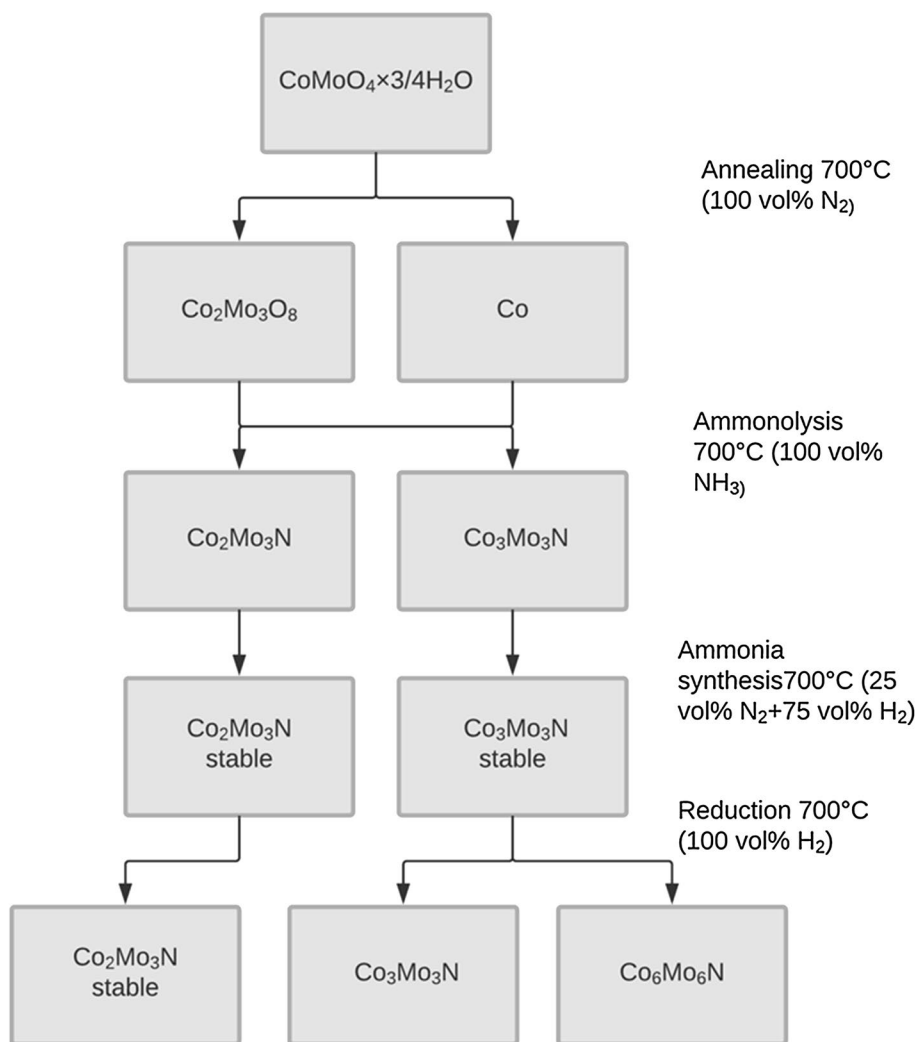

Fig. 7 Scheme of the transformations, which occurred during the process performed in the reaction chamber of the diffractometer

synthesis path. Ammonolysis of $NiMoO_4$ reported earlier (Bion et al. 2015) resulted in the formation of Ni_2Mo_3N phase, which is isostructural to Co_2Mo_3N. However, no phase similar to Co_3Mo_3N was identified. Also, intermediates were different; $Ni_{0.2}Mo_{0.8}N$, MoO_2 and metallic nickel were identified by X-ray diffraction. Ni_2Mo_3N activity was steady under 30-h ammonia synthesis test, which suggests that the catalyst is stable under this conditions. Under reduction conditions, Ni_2Mo_3N has not been transformed to nitrogen-lean phase like Co_6Mo_6N. The lattice nitrogen in the nickel-based catalyst is less reactive than in the cobalt-based counterpart. Apparently more studies are required to fully understand the structural and catalytic properties of this promising group of materials.

Conclusions

The precursor of the ammonia synthesis catalyst based on cobalt molybdenum nitrides is cobalt molybdate hydrate $CoMoO_4 \cdot 3/4H_2O$. The annealing of the precursor at 700 °C under nitrogen leads to the formation of $Co_2Mo_3O_8$ and metallic cobalt mixture. As a result of ammonolysis, a mixed cobalt molybdenum nitrides in the form of Co_2Mo_3N and Co_3Mo_3N phases are produced. This material is considered as an active phase of the catalyst. Co_2Mo_3N/Co_3Mo_3N mixture is stable under ammonia synthesis atmosphere even at a high temperature (700 °C). Exposure of the catalyst to pure hydrogen results in the transformation of Co_3Mo_3N to nitrogen-lean Co_6Mo_6N phase. Under these conditions, Co_2Mo_3N phase remains stable.

References

Bion N et al (2015) The role of preparation route upon the ambient pressure ammonia synthesis activity of Ni_2Mo_3N. Appl Catal A 504:44–50. https://doi.org/10.1016/j.apcata.2014.10.030

Dahl S, Logadottir A, Jacobsen CJH, Norskov JK (2001) Electronic factors in catalysis: the volcano curve and the effect of promotion in catalytic ammonia synthesis. Appl Catal A Gen 222:19–29

Gregory DH, Hargreaves JSJ, Hunter SM (2011) On the Regeneration of Co_3Mo_3N from Co_6Mo_6N with N_2. Catal Lett 141:22–26. https://doi.org/10.1007/s10562-010-0464-3

Hargreaves JSJ (2014) Nitrides as ammonia synthesis catalysts and as potential nitrogen transfer reagents. Appl Petrochem Res 4:3–10. https://doi.org/10.1007/s13203-014-0049-y

Hunter SM, McKay D, Smith RI, Hargreaves JSJ, Gregory DH (2010) Topotactic nitrogen transfer: structural transformation in cobalt molybdenum nitrides. Chem Mater 22:2898–2907. https://doi.org/10.1021/cm100208a

Jackson SK, Layland RC, Loye H-Cz (1999) The simultaneous powder X-ray and neutron diffraction refinement of two η-carbide type nitrides, Fe_3Mo_3N and Co_3Mo_3N prepared by ammonolysis and by plasma nitridation of oxide precursors. J Alloy Comp 291:94–101

Jacob KT, Vana Varamban S (1998) Phase equilibria and thermodynamic properties of ternary oxides in the system Co–Mo–O. J Alloys Compd 280:138–146. https://doi.org/10.1016/S0925-8388(98)00684-7

Jacobsen CJH (2000) Novel class of ammonia synthesis catalysts. Chem Commun. https://doi.org/10.1039/b002930k

Jacobsen CJH, Dahl S, Clausen BS, Bahn S, Logadottir A, Norskov JK (2001) Catalyst design by interpolation in the periodic table: bimetallic ammonia synthesis catalysts. J Am Chem Soc 123:8404–8405. https://doi.org/10.1021/ja010963d

Jarlborg T, Peter M (1984) Electronic structure, magnetism and Curie temperatures in iron, cobalt, and nickel. J Magn Magn Mater 42:89–99. https://doi.org/10.1016/0304-8853(84)90293-2

Kojima R, Aika K-i (2001a) Cobalt molybdenum bimetallic nitride catalysts for ammonia synthesis Part 1. Preparation and characterization. Appl Catal A Gen 215:149–160

Kojima R, Aika K-i (2001b) Cobalt molybdenum bimetallic nitride catalysts for ammonia synthesis Part 3. Reactant gas treatment. Appl Catal A Gen 219:157–170

McAulay K et al (2015) The influence of pre-treatment gas mixture upon the ammonia synthesis activity of Co–Re catalysts. Catal Commun 68:53–57. https://doi.org/10.1016/j.catcom.2015.04.016

Mckay D, Gregory DH, Hargreaves JSJ, Hunter SM, Sun X (2007) Towards nitrogen transfer catalysis: reactive lattice nitrogen in cobalt molybdenum nitride. Chem Commun. https://doi.org/10.1039/b707913c

Moszyński D (2013) Controlled phase composition of mixed cobalt molybdenum nitrides. Int J Refract Met Hard Mater 41:449–452. https://doi.org/10.1016/j.ijrmhm.2013.06.002

Moszyński D, Jędrzejewski R, Ziebro J, Arabczyk W (2010) Surface and catalytic properties of potassium-modified cobalt molybdenum catalysts for ammonia synthesis. Appl Surf Sci 256:5581–5584. https://doi.org/10.1016/j.apsusc.2009.12.150

Moszyński D, Adamski P, Pełech I, Arabczyk W (2015) Katalizatory kobaltowo-molibdenowe domieszkowane cezem do syntezy amoniaku (Cobalt-molybdenum catalysts doped with cesium for ammonia synthesis). Przem Chem 94:1399–1403. https://doi.org/10.15199/62.2015.8.31

Moszyński D, Adamski P, Nadziejko M, Komorowska A, Sarnecki A (2018) Cobalt molybdenum nitrides co-promoted by chromium and potassium as catalysts for ammonia synthesis. Chem Pap 72:425–430. https://doi.org/10.1007/s11696-017-0292-7

Prior TJ, Battle PD (2003) Facile synthesis of interstitial metal nitrides with the filled β-manganese structure. J Solid State Chem 172:138–147. https://doi.org/10.1016/S0022-4596(02)00171-8

Tarka A, Zybert M, Truszkiewicz E, Mierzwa B, Kępiński L, Moszyński D, Raróg-Pilecka W (2015) Effect of a barium promoter on the stability and activity of carbon-supported cobalt catalysts for ammonia synthesis. ChemCatChem 7:2836–2839. https://doi.org/10.1002/cctc.201500309

Tarka A, Zybert M, Kindler Z, Szmurło J, Mierzwa B, Raróg-Pilecka W (2017) Effect of precipitating agent on the properties of cobalt catalysts promoted with cerium and barium for NH_3 synthesis obtained by co-precipitation. Appl Catal A 532:19–25. https://doi.org/10.1016/j.apcata.2016.11.030

Tourne G, Czeskleba H (1970) Formation and properties of a $Zn_2W_3O_8$ phase and of sodium solutions of the formula$[M(II)]Mo_{8-X}W_XO_8$ (M = magnesium, manganese, iron, cobalt, nickel, zinc, and cadmium). C R Acad Sci Ser C 271:136–138

Zybert M, Tarka A, Mierzwa B, Kępiński L, Raróg-Pilecka W (2016) Promotion effect of lanthanum on the Co/La/Ba ammonia synthesis catalysts—the influence of lanthanum content. Appl Catal A 515:16–24. https://doi.org/10.1016/j.apcata.2016.01.036